In vivo effects of Cisplatin and titanium dioxide nanoparticles combined treatment

ABSTRACT

Cisplatin, the first metal-based chemotherapeutic drug, remains widely used in treating various solid cancers despite its side effects and drug resistance. Researchers have explored combining Cisplatin with multiple substances to overcome its limitations. Different nanoparticles have been studied with Cisplatin. We examined the in vivo effects of orally administered Cisplatin (50 µg/ml) and titanium dioxide nanoparticles ($NPTiO_2$, 50 µg/ml), both alone and in combination, in D. melanogaster. In this context, Drosophila melanogaster serves as a valuable alternative model for assessing the toxicity of many substances and diseases like cancer, Alzheimer's, and alcoholism. We investigated whether co-exposure to cisplatin and $NPTiO_2$ induces synergistic transcriptional repression in vivo. Using RNA-seq and bioinformatics analyses, we evaluated gene modulation to assess toxic effects in each experimental group. We found that flies treated with either cisplatin or $NPTiO_2$ alone showed gene modulation associated with non-toxic substance processing. However, the group treated with both cisplatin and $NPTiO_2$ showed a limited number of Differentially Expressed Genes (DEGs) and disruptions in cell division and DNA/RNA metabolism. Mortality rates remained statistically unchanged across all groups. These findings suggest that co-exposure to Cisplatin and $NPTiO_2$ causes transcriptional repression and disruption of critical cellular pathways, indicating potential impairments in cellular function.

INTRODUCTION

Cisplatin is the commercial name for the compound (SP-4-2)-diamminedichloridoplatinum (II), the first metal-based anticancer drug widely used to treat several cancers. Multiple *in vitro* and *in vivo* studies have shown its mechanism of action, which involves the generation of DNA lesions. These lesions trigger several signal transduction pathways that inhibit replication and transcription, cell cycle arrest, DNA repair, and apoptosis (Ghosh, 2019). The DNA damage results from Cisplatin's interaction with the purine bases on DNA, generating DNA interstrand adducts (G-G,

60%; A-G, 20%), as well as DNA-protein interactions. In humans, polymorphisms in genes responsible for DNA adduct repair, such as ERCC2 and XPC, as well as genes related to membrane pumps, drug efflux, or detoxifying genes (ACYP2, ABCC3, COMT, TPMT), are associated with ototoxicity (Karasawa; Steyger, 2015). Here, we investigate the *in vivo* impact of Cisplatin and its interactions with cellular processes. A genotoxic study using the Comet assay indicates that in *D. melanogaster*, DNA damage detected has higher levels of G–G cross-links than G monoadducts. This way, G-G cross-links in *D. melanogaster* contribute to the induction of DNA strand breaks, through both the blockage of DNA replication and repair; not all Cisplatin-induced adducts contribute to generating DNA strand breaks (García Sar *et al.*, 2012). The upregulated TIMELESS gene, a human homologue of the D. melanogaster Tim gene related to circadian rhythm and cell cycle checkpoints, was demonstrated *in vitro* (in NPC cell lines) and *in vivo* to confer resistance to Cisplatin-induced apoptosis via the Wnt/β-catenin pathway (Liu *et al.*, 2017).

Groen *et al.* performed a survivor assay demonstrating that Cisplatin has dose-dependent toxicity associated with reduced survival of *Drosophila*. In this assay, the authors demonstrated that *Drosophila* treated with Cisplatin at concentrations ranging from 10 to 50 µg/ml, diluted in the culture medium, exhibited a relative increase in the activation of genes associated with reactive oxygen species (ROS) in the axonal mitochondria. They also demonstrate that flies with the glutathione peroxidase gene silenced by RNA interference (RNAi) exhibit reduced sensitivity to Cisplatin compared to wild-type flies. It highlights the fruit fly's usefulness as a model organism for *in vivo* studies of chemotherapy-induced peripheral neuropathy (CIPN) (GROEN, 2022). In this sense, previous data suggest that phagocytosis metabolism is affected in Cisplatin-treated PC12 cells, which decreases membrane lipid content, thereby affecting exocytosis and altering apoptosis metabolism (Mohammadi, Li, Ewing, 2018). Different carriers have been used to reduce Cisplatin's side effects. In this context, the combined use of 50 mg/ml of NPTiO2 and 10 µg/ml of Cisplatin improved chemotherapy response *in vitro* in the F10 melanoma model and *in vivo* in C57BL/6 mice. The induction of autophagy induced by the nanoparticles played a crucial role in sensitizing F10 melanoma cells (Adibzadeh *et al.*, 2021).

Although largely used in food, pharmaceutical, and cosmetic industries, titanium dioxide nanoparticles ($NPTiO_2$) have *in vivo* side effects that are still unconfirmed. An

in vivo test using the bivalve *Mytilus galloprovincialis* exposed to 1, 10, or 100μgL^{-1} of $NPTiO_2$ shows lysosomal and oxidative stress biomarkers altered, and the transcription level of immune-related antioxidant genes decreases (Barmo *et al.*, 2013). Mice orally treated with $NPTiO_2$ at 5, 50, or 500 mg per kg body weight dosage for five consecutive days, and sacrificed 24h after treatment, showed persistent apoptotic DNA fragmentation and mutations in p53 exons at one or two weeks after treatment. They also exhibit persistent elevations in malondialdehyde and nitric oxide levels, as well as decreases in glutathione levels and catalase activity, compared to the control mice in a dose- and time-dependent manner.

$NPTiO_2$ administration is directly related to persistent inflammation, apoptosis, and oxidative stress, as well as the induction of chronic gastritis (Mohamed, 2015). Additionally, it directly binds to proteins involved in cellular functions, resulting in primary genotoxic effects. The main mechanism of this $NPTiO_2$ genotoxic effects was demonstrated to be caused by reactive oxygen species (ROS) generated by an increase in H_2O_2, singlet oxygen, and lipid peroxide levels, which cause a reduction in glutathione (GSH) and antioxidant levels (Wani; Shadab, 2020). Additionally, a study examining 34 robust datasets does not support a direct DNA-damaging mechanism for TiO2 in either the nano or micro form (Kirkland *et al.*, 2022).

Here, we investigate the *in vivo* effects of oral administration of Cisplatin (50μg/ml) and TiO_2 nanoparticles (50μg/ml) isolated and in combination in *Drosophila melanogaster*. Furthermore, we analyze gene modulation by identifying differentially expressed genes (DEGs) obtained through RNA-seq. Additionally, we conducted downstream analysis to verify the ontology terms associated with these different treatments in *Drosophila*. Our data shows a specific expression pattern in flies treated with Cisplatin and TiO_2 nanoparticles simultaneously, presenting an intermediate transcript level with a minimal number of upregulated DEGs.

MATERIALS AND METHODS

1. *Drosophila melanogaster* maintenance

Drosophila melanogaster strain Oregon (RRID:BDSC.5) was obtained from the Bloomington *Drosophila* Stock Center, Indiana University. The culture was performed in standard cornmeal-yeast-agar medium (Brent; Oster, 1974) and maintained in an incubator at 25 °C with humidity between 70% and 80% and a 12-hour light cycle.

2. Treatments

One- to four-day-old D. melanogaster strain Oregon flies were divided into four groups, each containing 30 individuals. Each group consists of a 4:1 female-to-male ratio. The control group was treated with a standard medium enriched with a mixture of yeast, water, and a green food coloring dye. Treatment groups were treated as follows: CIS group – water was substituted by an aqueous Cisplatin solution (50μg/ml); NPTIO2 group - water solution was substituted by an aqueous TiO_2 solution (50μg/ml); CIS_NPTIO2 group – water was substituted by Cisplatin water solution (50μg/ml) and $NPTiO_2$ water solution (50μg/ml) concomitantly. All treatments were performed in triplicate. Flies were kept in this condition for 3 (three) days.

3. Preparation of Used Solutions

$NPTiO_2$ water solution was prepared using 50μg/ml of TiO_2 (Sigma-Aldrich, Cat. No.: 718467; nano powder, 21 nm primary particle size (TEM), ≥99.5% trace metals basis), which was heated in an oven (200ºC) for 30 minutes. Then, TiO_2 was solubilized in deionized water by sonication (25ºC, 20 minutes). Cisplatin (Cat. No.: PHR1624) obtained from Merck was dissolved in Milli-Q water (18.2 MΩ cm distilled deionized water obtained from a Milli-Q system, Millipore, Bedford, MA, USA), forming a 50μg/ml Cisplatin solution.

4. Survival analysis

Kaplan-Meier then calculated the survival rate, and survival analysis, followed by the Log-rank (Mantel-Cox) test, was performed in R Studio using the “survival package”. After that, a phenotypic analysis was conducted using a stereoscope to verify any possible phenotypic alterations resulting from the treatments.

5. RNA isolation

We used Trizol™ reagent (ThermoFisher™ Scientific, Waltham, Massachusetts, USA) to isolate total RNA from two female flies from each treated group (CIS group, NPTIO2 group, and CIS_NPTIO2 group) and the control group, according to the manufacturer’s instructions. The RNA isolation was performed using the whole animal. To avoid DNA contamination, we used the RNase-Free DNase Set (QIAGEN, Cat. No.: 79254) according to the manufacturer's instructions. Then, RNA was collected after ethanol precipitation. RNA quality was analyzed using agarose gel visualized in Molecular Imager® Gel Doctm XR+ Imaging system (Bio-Rad Laboratories, Inc.) and

quantified with NanoDrop 2000 spectrophotometer (ThermoFisher™ Scientific) and a QuBit 3.0 Fluorometer (ThermoFisher™ Scientific).

6. RNA-seq

RNASeq library preparation and sequencing were performed at Computational Genomics Unity Darcy Fontoura de Almeida (UGCDFA) of the National Laboratory of Scientific Computation (LNCC) (Petrópolis, RJ, Brazil). The mRNA sequencing libraries were constructed using Illumina Stranded mRNA Prep Ligation kit (Illumina, San Diego, CA, USA), according to the manufacturer's protocol. The quality of libraries was verified using Agilent TapeStation 4200 System (Agilent Technologies, USA) according to the manufacturer's instructions. Sequencing was conducted on an Illumina NextSeq 500 platform (Illumina, San Diego, CA, USA) using the NextSeq 500/550 high-output kit v2.5 (150 cycles) (Illumina, USA), generating reads of 2 × 75 bp.

7. Sample processing

The quality of the sequenced libraries was analyzed using the FastQC software (Wingett; Andrews, 2018). Adapters, sequences, and low-quality regions were filtered using Trimmomatic Version 0.36 (Bolger, Lohse, and Usadel, 2014). The remaining readings were aligned to the reference genome of *Drosophila melanogaster* (ASM2977511v1, date: April 17, 2023), using the BWA mapper (Li; Durbin, 2009). The alignments' quality was analyzed using the Samtools tool (Li *et al.*, 2009), and the count of mapped reads was performed with the HT-seq Count tool (Anders, Pyl, Huber, 2015).

All codes are available in:
https://github.com/CristianoNCosta/CristianoNCosta.git

8. Quantification and analysis of differential gene expressions

We used R environment tools to run the edgeR tool for read count normalization and differential gene expression analysis (Robinson; McCarthy; and Smyth, 2010). Tools from the BiocManager package were used: DESeq2 tool (Love, Huber, was used to compare the results using > $\log^2$ FC cutoff |1,0| and p-value adjusted (p_{adj}) < 0,05. RNA-seq expression values are in Log 2-fold change (Log2fc); the control was set as 1, and the treatment at the Log2fc respective value greater than 1 (Log2fc values and standard errors are supplied (*Supplementary Table 1*).

9. Data downstream analysis

Downstream analysis of differentially expressed genes (DEGs) obtained in the previous step. Then, a functional enrichment analysis of DEGs was performed. R statistical package environment was used, also databases like FlyBase (Öztürk-Çolak *et al.*, 2024), FlyEnrichr (Kuleshov *et al.*, 2019), Gene Ontology (GO) (The Gene Ontology Consortium, 2019), among others—data supplied in the annexed *Supplementary Table 2*.

RESULTS AND DISCUSSION

To evaluate the effects of individual and combined administration of Cisplatin (50 µg/ml) and TiO_2 nanoparticles (50 µg/ml) *in vivo*, we measured the mortality rates of *Drosophila* melanogaster using the described experimental protocol (Materials and Methods). The survival rate was calculated by comparing flies from each treated group against the control group (CG) using the Kaplan-Meier method, followed by the Log-rank (Mantel-Cox) test (Figure 1). We found no significant variation among all considered groups (p = 0,76).

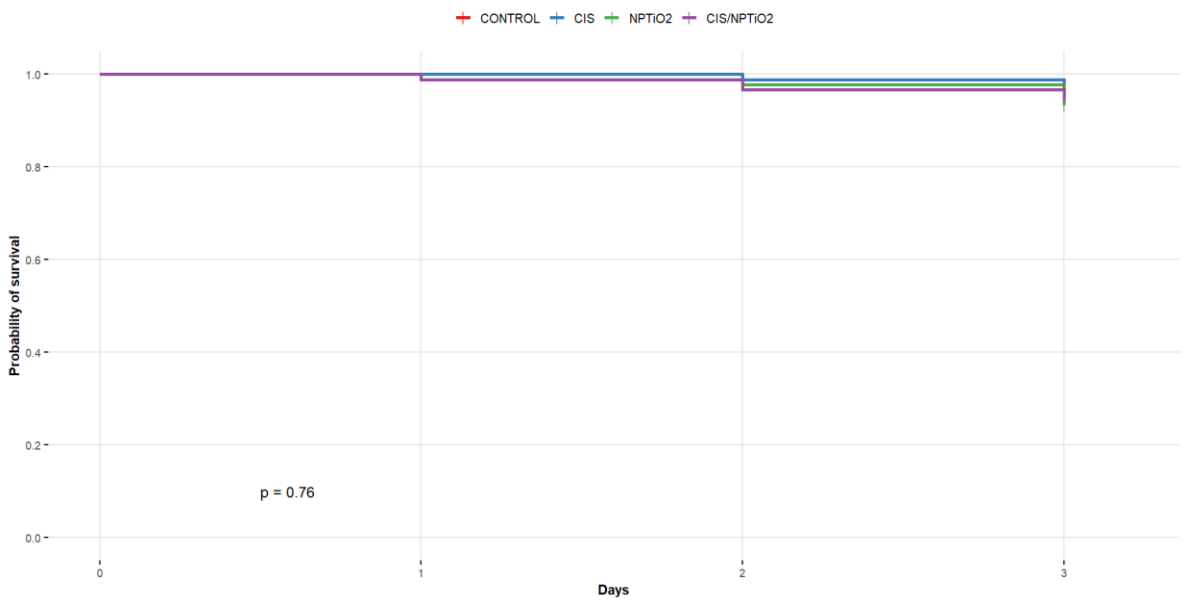

Figure 1: Kaplan–Meier survival curves of *Drosophila* melanogaster exposed to different treatments: control, Cisplatin (50 µg/ml CIS), titanium dioxide nanoparticles (50 µg/ml NPTIO2), and the combination CIS/NPTIO2 (50 µg/ml/50 µg/ml). Survival rates were similar across all experimental groups (p = 0.76). The Log-rank (Mantel–Cox) test showed no statistically significant differences among the groups (Events: 18; p-value: 0.75347), indicating that none of the treatments significantly affected fly survival over the 3-day observation period.

To check for possible variance among the data obtained in DESeq, we performed a Principal Component Analysis (PCA) on the gene expression levels of each group.

PCA is widely used to analyze variance in data. This analysis suggests that CIS_NPTIO22 is an outlier sample (Figure 2).

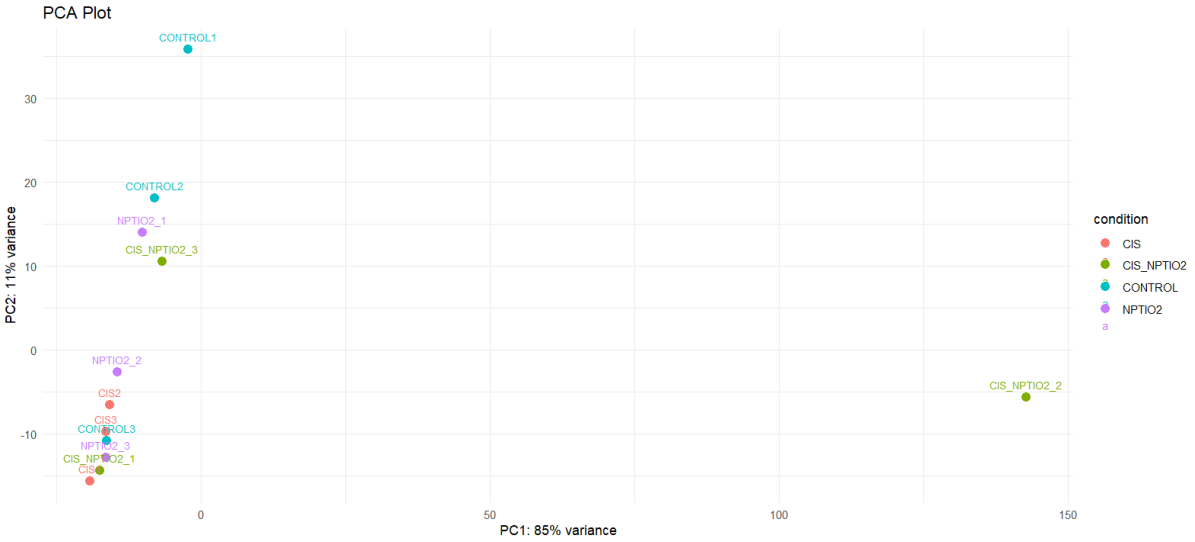

Figure 2. PCA plot of RNA-seq data (rlog-normalized) showing sample separation by treatment: controls (black) cluster on the left, while CIS (red), CIS_NPTIO2 (green), and NPTIO2 (purple) form distinct groups along PC1 (85% variance). PC2 explains minimal variation (11%). CIS_NPTIO22 exhibits an intermediate profile among CIS and NPTIO2.

In the BiocManager package, the standard PCA implemented by the DESeq2 package uses the *regularized logarithm* (rlog) as the normalization method. rlog applies a variance-stabilizing log transformation tailored for count data, focusing on biological interpretability. Robust Scaler is another normalization method that standardizes data using median and interquartile range (IQR), making it resistant to and of general applicability (not RNA-seq-specific), prioritizing statistical robustness. For this reason, we perform another PCA analysis combining both normalization methods (rlog first, then Robust scaling) to optimize PCA results by balancing variance stabilization and outlier resilience.

Figure 3 and Table 1 present the data obtained from the robust PCA. Figure 3 is a heatmap with a dendrogram on the top side. The dendrogram reveals the gene expression profiles of the samples based on the similarity of their expression patterns across the top 10,000 most differentially expressed genes. The most precise observation of Figure 3 reveals some variance between samples from the CONTROL group; also, there is variance in samples from the treated groups (CIS and NPTIO2). However, there is a significant difference between samples from the CIS_NPTIO2 group, specifically CIS_NPTIO22, and other samples within the same group.

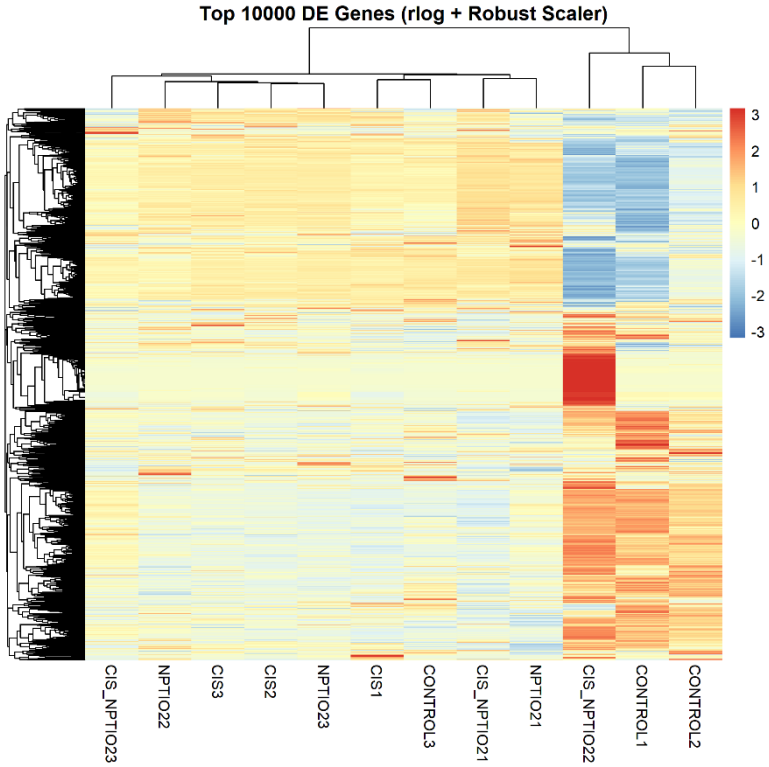

Figure 3: Heatmap from Principal Component Analysis (PCA) of rlog + Robust Scaler normalized RNA-seq data showing the transcriptome pattern of samples from the different experimental groups (CONTROL, CIS, $NPTiO_2$, CIS_$NPTiO_2$) of biological triplicates (n=3/group).

Table 1: Euclidean Distance between CIS_NPTIO22 sample and other samples. Scale units in standard deviation (Robust Scaler).

CIS1	CIS2	CIS3	CIS_NPTIO21	CIS_NPTIO23	
4974.11	4949.75	4944.15	4950.60	4940.42	
CONTROL1	**CONTROL2**	**CONTROL3**	**NPTIO21**	**NPTIO22**	**NPTIO23**
4919.46	4926.30	4950.49	4948.30	4943.52	4933.49

Table 1 shows the Euclidean distance between CIS_NPTIO22 and all other samples. Figure 3 illustrates the transcriptomic profile changes in response to CIS_NPTIO2 treatment, suggesting that the combination treatment (CIS + NPTiO2) produces a distinct and consistent gene expression signature.

We then performed a quantitative analysis to verify the Euclidean distance among the replicates. Figure 4 shows that CIS_NPTIO22 has a distance greater than 4000 Standard Deviation (SD) among other CIS_NPTIO22 replicates, and similar distances are observed for all samples from any other treatment group. These data are consistent with the outlier condition of CIS_NPTIO22, indicating that this sample should be excluded from further analysis to maintain data integrity. The data from

Figure 3 and Table 1 collectively support the hypothesis that CIS_NPTIO22 is an outlier.

After outlier removal, we repeat the PCA and quantitative analysis to verify the Euclidean distance among the replicates. Figure 4 shows a 70% variance in PC1 and an 8% variance in PC2. Distances in PC2 among samples from the same group suggest potential minor biological variations within the same group. Notwithstanding this, across the PC1 axis, the most variable group is the CONTROL group. CONTROL3, which is approximately 40% distant from CONTROL1 and CONTROL2, which are compatible with biological variance. Nonetheless, the CONTROL group is still helpful for comparing transcription variance in all treatment groups. Figure 4 also points out that the most homogeneous samples are from the CIS group, which are closer to each other in both PC1 and PC2, suggesting that these samples form a distinct cluster. In the meantime, PC1 shows a heterogeneous response among different samples from the same treatment groups. NPTIO21 is about 15% distant from NPTIO22 and NPTIO23, and CIS_NPTIO21 is distant from CIS_NPTIO23. These data demonstrate biological variation among samples of these groups, but these variations are not drastic enough to discard the samples. Additionally, distances in PC1 reveal the most significant biological variance between samples in the CONTROL group, indicating a treatment effect, with a primary separation among the CIS, NPTIO2, and CIS_NPTIO2 groups from the CONTROL group.

To confirm those mentioned above, we computed the Euclidean distance among the replicates after outlier removal, and neither the control nor the treated group has a distance greater than 750 from any other replicate, confirming that there are no other outliers (*Supplemental material 01*). These data suggest a possible synergistic effect of CIS_NPTIO2 treatment compared to the administration of CIS and NPTIO2 separately.

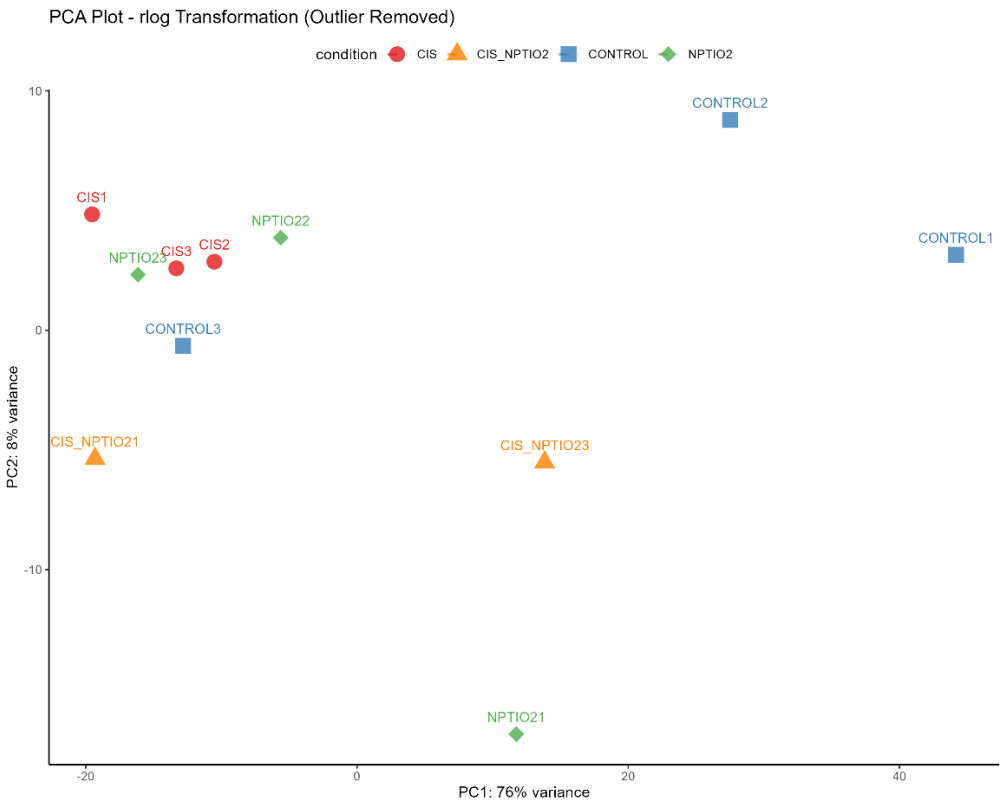

Figure 4: Two-dimensional PCA projection of rlog-transformed count data following quality control and outlier removal. Variance explained: PC1 (76%), PC2 (8%). Ellipses represent 95% confidence intervals for each experimental group. The improved cluster compactness and inter-group separation compared to pre-filtered data confirm the effectiveness of outlier removal in enhancing data quality and analytical robustness.

Samples are colored by experimental condition: CONTROL (blue), CIS (red), CIS_NPTIO2 (orange), and NPTIO2 (green). The analysis demonstrates a clear separation between treatment groups following outlier exclusion.

Taken together, these statistical analyses demonstrate that removing the CIS_NPTIO22 outlier leads to greater consistency across biological replicates and supports robust inference about treatment effects, allowing for more reliable downstream comparisons and interpretation.

Expanding upon these findings, we next examined the global patterns of gene expression and differential regulation elicited by each treatment group.

Figure 5 shows Volcano plots with the distribution of differentially expressed genes (DEGs) of each challenged group (CIS, NPTIO2, and CIS_NPTIO2) compared with the control. Each dot represents a gene; black denotes non-significant changes, and red denotes DEGs with significant fold changes. ($\log_2 fc > |1.0|$ and $p_{adj} < 0.05$), and Figure 6 shows the total volume of transcripts by each control or treatment group.

Comparing the treatment groups with the CONTROL group, our data shows that both the CIS and CIS_NPTIO2 groups significantly increased the total transcript count. However, the NPTIO2 treatment alone appears to have a less pronounced effect, yet still presents a higher total transcript count than the control group, as demonstrated by its slightly higher median value. Although it presented a lower number of upregulated and downregulated DEGs, the CIS_NPTIO2 group had a marginally higher transcript count than the CIS group alone and, more importantly, showed much less variability, suggesting CIS_NPTIO2 has more stable or robust effect of the combination of Cisplatin (50 μg/ml) and TiO_2 nanoparticles (50 μg/ml) causes an intermediate effects in animals treated in this way.

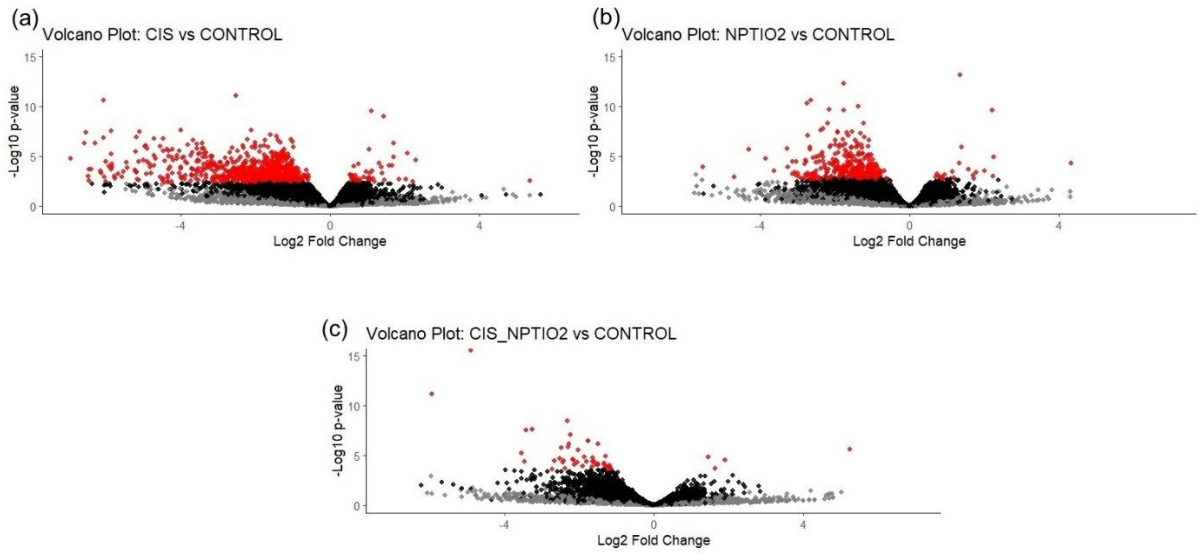

Figure 5: Differential gene expression analysis. Volcano plots display the relationship between statistical significance (-$\log_{10}$ p-value) and the magnitude of change ($\log_2$ fold change) for all measured genes. (a) CIS treatment versus CONTROL, (b) NPTIO2 treatment versus CONTROL, (c) CIS_NPTIO2 treatment versus CONTROL. DEGS with differentiated expression (fold change (log2fc > |1.0| and p-Value <0.05): Significant (•), Not significant (•).

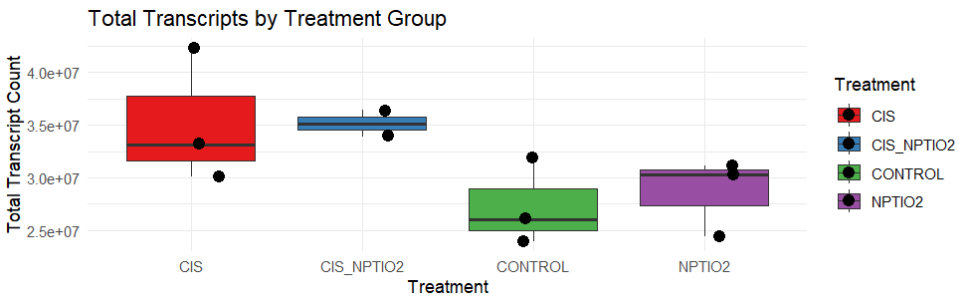

Figure 6 - Total Transcript Counts by Treatment Group: Box plots show the total transcript counts for each of the four treatment groups (CIS, CIS_NPTIO2, CONTROL, and NPTIO2). The line within each box indicates the median value, with the box representing the interquartile range (IQR). Black dots represent individual sample data points. Total transcript counts are highest in the CIS and CIS_NPTIO2 treatment groups, while the CONTROL group shows the lowest counts.

After confirming the statistical data and outlier removal, we began to analyze the DEGs in each group. The Venn diagram (Figure 7) indicates the total number of DEGs obtained by each group isolated and those DEGs found in two or more groups. It shows that there are two upregulated DEGs detected in all groups (*CG10013*, *aqz*). CIS and NPTIO2 groups have four upregulated DEGs (*CG11263*, *CG18088*, *Tango6*, *inaF-D*) and one long non-coding RNA (lncRNA:CR43836). One upregulated DEG was identified in the CIS and CIS_NPTIO2 groups (CG5568), and the NPTIO2 and CIS_NPTIO2 groups had one upregulated DEG (*CG3213*). Conversely, treatment conditions generate a different profile of downregulated DEGs in each group. Additionally, a larger number of DEGs were downregulated; only a few DEGs were downregulated by both the CIS_NPTIO2 group and the NPTIO2 or CIS groups separately, or by all treated groups simultaneously. Additionally, we identified a large number of DEGs that both the CIS and NPTIO2 groups simultaneously downregulated.

The reduced number of up- and downregulated DEGs, specifically in the CIS_NPTIO2 group, suggests a possible synergistic effect of cisplatin and TiO2 nanoparticles administered simultaneously to the *Drosophila*. This observation aligns with what was previously described by Adibzadeh and colleagues. (2021) in murine melanoma models, and probably, is caused by a reduction in cell signaling processes due to the joint administration of these substances in *Drosophila*.

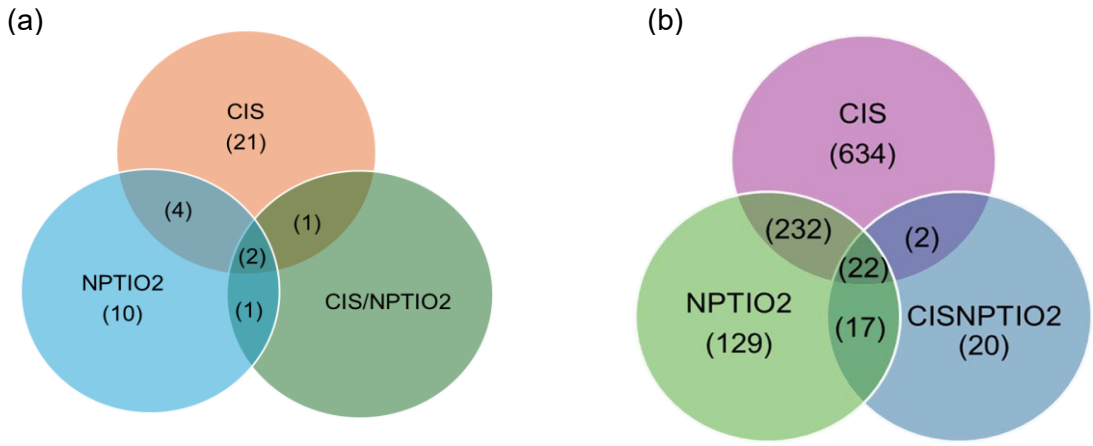

Figure 7: Venn diagram relative to the number of DEGs obtained in (a) upregulated DEGs and (b) downregulated DEGs in the challenged groups.

Downstream analysis of upregulated DEGs detected in flies treated with 50μg/ml Cisplatin, hereinafter referred to as the CIS group, shows no significant KEGG pathway, but presents 24 upregulated DEGs and three long non-coding RNA (Figure

8). The upregulated DEGs in the CIS group have GO terms for biological processes (BP) related to response to stimulus, development, biogenesis, DNA metabolism, and immune response. GO terms for molecular function (MF) corresponding to enzyme, metal ion binding, RNA binding, carbohydrate binding. Still, these DEGs have cellular component (CC) GO terms related to the membrane, cell periphery, cytosol, nucleus, and other cellular components. (*Supplementary Table 1)*. This data indicates that *Drosophila* treated with 50μg/ml Cisplatin activates metabolism in response to a stimulus and the DNA repair machinery. It is distinct from previous data, which identify DEGs upregulated only at higher cisplatin concentrations (Mombach *et al.*, 2022).

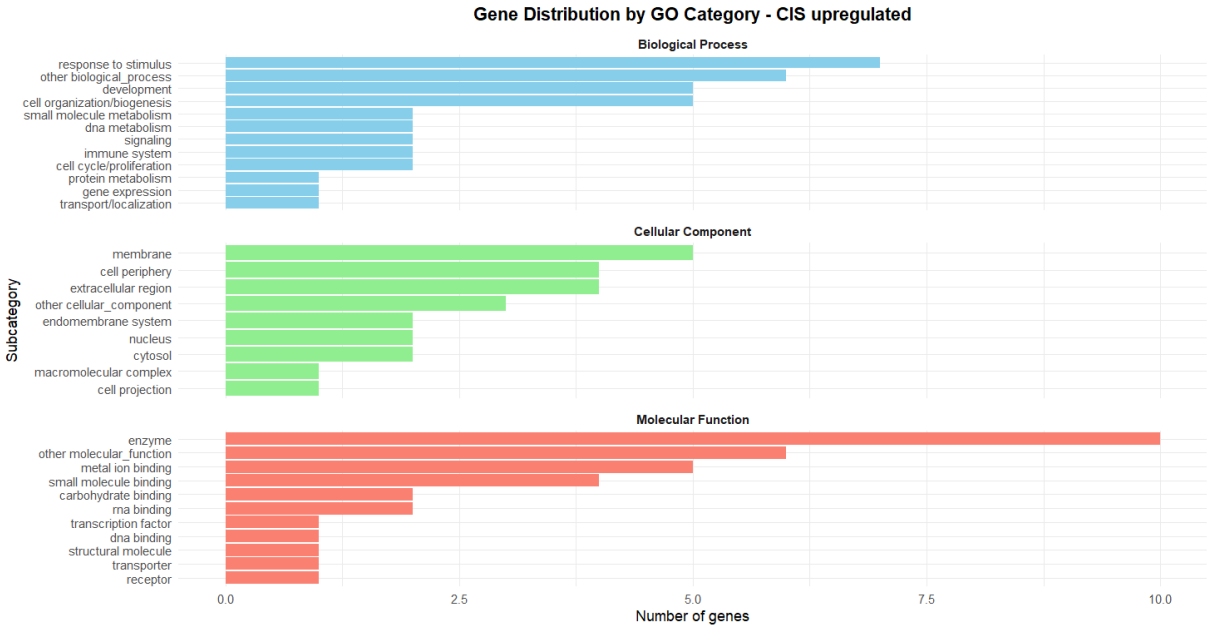

Figure 8 - GO enrichment analysis of upregulated genes under CIS treatment: (■) Biological Process, (■) Cellular Component, and (■) Molecular Function. The full results are presented in Supplementary Table 1. Data source GO Summary Ribbon (Fly Base).

Flies treated with 50μg/ml of $NPTiO_2$ (NPTIO2 group) exhibit upregulation in 16 DEGs and one long non-coding RNA. 2 DEGs are also upregulated by all treatment groups, 4 DEGs are shared with CIS group, and one DEG is at the same time upregulated by CIS_NPTIO2. These DEGs are related to 10 biological processes (gene expression, protein metabolism, development, signaling, response to stimulus, etc.); 6 molecular functions (small molecule binding, RNA binding, transport, enzyme, receptor binding), and nine cellular components (macromolecular binding, nucleus, membrane, chromosome, endomembrane system) (Figure 9). This NPTIO2 group, our data is in accordance with previous data, showing that gene expression is not affected

by $NPTiO_2$ uptake, and activation occurs in DEGs related to response to stimulus and transport/cell localization (Jovanović; Cvetković; Mitrović, 2016).

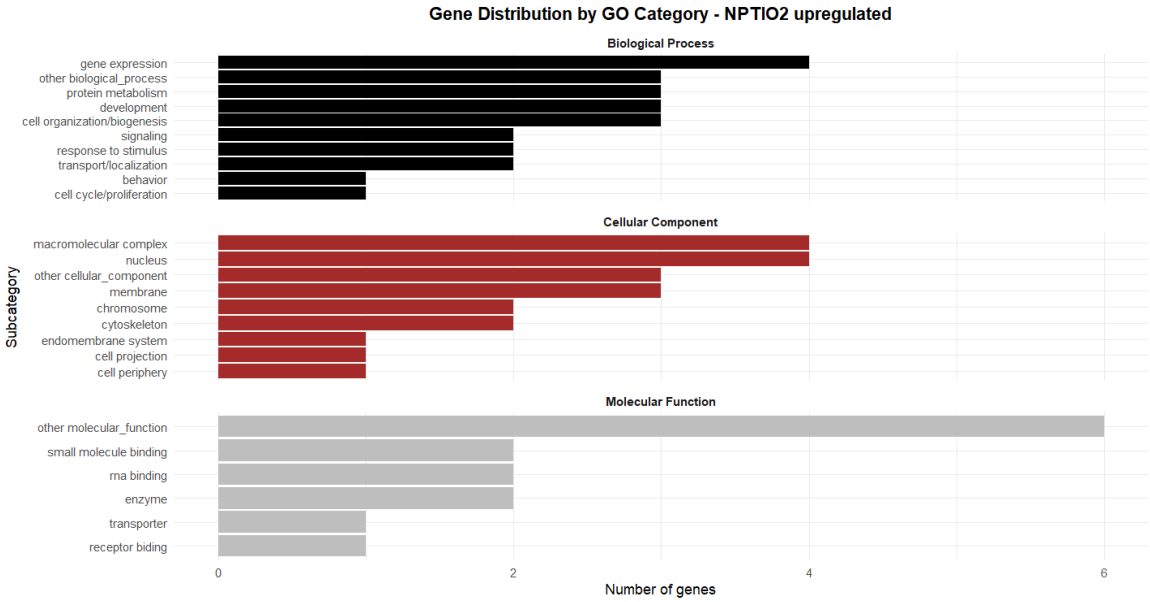

Figure 9: **GO enrichment analysis of upregulated genes under NPTIO2 treatment**: (■) Biological Process, (■) Cellular Component, and (■) Molecular Function. Full results are in Supplementary Table 1. Data source GO Summary Ribbon (Fly Base).

Finally, Table 2 shows four upregulated DEGs observed in the CIS_NPTIO2 group (flies treated with 50μg/ml of Cisplatin and 50μg/ml of $NPTiO_2$ concomitantly). We demonstrate that $NPTiO_2$ activates cytoskeleton and lipid metabolism genes, which are typically repressed in flies treated only with Cisplatin, but are active in flies treated with nanoparticles in general (Adibzadeh *et al.*, 2021; González-López *et al.*, 2020; Mohammadi *et al.*, Li). As these genes are related to endocytosis, this suggests a possible increase in the incorporation of Cisplatin due to the effect of $NPTiO_2$ when administered jointly.

Table 2: Gene Ontology (GO) enrichment analysis of CIS_NPTIO2-upregulated genes

GO Category	Subcategory	Nº Genes
Cellular Component	cytoskeleton	1
	nucleus	1
Biological Process	fatty-acyl-CoA biosynthetic process	1
	long-chain fatty acid metabolic process	1

GO Category	Subcategory	Nº Genes
	biological_process	1
Molecular Function	enzyme	1

Table 2: DEGs from CIS_NPTIO2 group classified using GO Summary Ribbon (Fly Base). Only the most specific terms are shown. Complete data available in Supplementary Table 1.

We identified two genes that were upregulated in all three treatment groups: *CG10013* and *aqz*. *CG10013* codes for a ubiquitin-conjugating enzyme E2-binding protein that accepts ubiquitin from specific E2 ubiquitin-conjugating enzymes, and transfers it to substrates, generally promoting their degradation by the proteasome. CG10013 contributes to genome structural dynamics in *Drosophila* (Bastide *et al.*, 2016). The gene *aqz* is predicted to be active in the nucleus and codes for the Aaquetzalli protein isoform A. *aqz* (Mendoza-Ortíz; Murillo-Maldonado; Riesgo-Escovar, 2018). Together, CG10013 and *aqz* play a role in responses to oxidative stress and other conditions that affect the cell and are expected to be upregulated in flies of all treated groups.

CG5568 is regulated in flies from both CIS and CIS_NPTIO2 groups. This gene is involved in the transcriptional regulation of the cell cycle, acting as a zinc finger protein that binds to DNA and has a role in eye development (Morrison *et al.*, 2006). Additionally, CG5568 is highly expressed in female germline cells and is involved in the fatty-acyl-CoA biosynthetic process (Li *et al.*, 2022). Upregulation of CG5588 is expected due to the protein-rich diet, which leads to activation of mitosis, despite cisplatin treatment.

CG3213 is upregulated in flies from both NPTIO2 and CIS_NPTIO2 groups; this gene is involved in ribosomal and protein translation (Pospisilik *et al.*, 2010). Also, *CG3213* was identified in a genome-wide screen for obesity-related genes in *Drosophila,* and a single-nucleotide polymorphism (SNP) in *CG3213* is associated with variation in starvation resistance (Mackay *et al.*, 2012). A screening performed in adult flies, including both sexes, demonstrates that triglyceride levels, a direct measure of adiposity, were determined in adult flies following RNAi induction. Inhibition of *CG3213* in muscle cells was shown to regulate triglyceride levels (Garlovsky; Sandler; Karr, 2022). Yet, *CG3213* is related to distinct processes in the germline stem cell lineage(Matsuoka *et al.*, 2017). Upregulation in DEGs related to fatty-acid and lipid metabolism in flies treated with TiO2 nanoparticles ($NPTiO_2$) is expected.

DEGs upregulated by the CIS_NPTIO2 group alone or simultaneously in one or the other two treated groups are related to biological processes described in Table 2. This data strongly suggests a possible increase in the incorporation of Cisplatin due to the rise in endocytosis mediated by the $NPTiO_2$ joint administration.

Drosophila from both CIS and NPTIO2 groups have three upregulated DEGs in common (*CG11263*, *CG18088,* and *InaF-D*) and an upregulated long non-coding RNA (lncRNA:CR43836). Recent data suggest that long non-coding RNAs (lncRNAs) may have essential regulatory functions in the genome (Zhong *et al.*, 2020). Specifically about the lncRNA:CR43836, data show this lncRNA is expressed in many embryonic tissues, larval visceral muscle cells, and adult females (Matthews *et al.*, 2015). *CG11263* is an RNA-binding protein related to lipid binding, cilium assembly, and intracellular transport, expressed in *Drosophila* embryos, prepupa, and pupa stages, and in adult females (ADAMS, 2000). Upregulation in *CG11263* could explain the presence of lncRNAs in treated flies in these groups, due to its role in transcription regulation. *CG18088* is related to *Drosophila's* immune response to *Wolbachia sp*, affecting transduction-related genes. *InaF-D* binds to the transient receptor potential (TRP) calcium channel and affects metal absorption (Chen; Montell, 2020). The last to DEGs are also related to immune response and metal response and are expected to be upregulated in flies treated with those metal compounds.

All flies were kept for three days, fed on food supplemented with wet yeast paste containing cisplatin, TiO_2 nanoparticles, or both substances concomitantly, without previous starvation. This can positively affect cell proliferation in both the control group and the treated groups, regardless of the group to which they belong. Several studies have demonstrated that protein intake affects tumor growth and oogenesis in female ovaries; therefore, the observation of upregulated DEGs related to this function is expected (Matsuoka et al., 2017; Lushchak; Strilbytska; Storey, 2023; Sun; Nystul; Zhong, 2023).

Previous studies have demonstrated that mated females can store sperm transcripts in their spermatheca, and the RNAs of sperm-related genes, including those of accessory gland and seminal fluid proteins, can be detected (Cridland; Begun, 2023; Prokupek *et al.*, 2008). Our treatment conditions, time of feeding, food supplementation provided to the flies, and the use of mated females could explain the difference between our results and those of the previous study in flies treated with the same Cisplatin concentration (Mombach *et al.*, 2022). Additionally, it could explain the

identification of DEGs that are primarily related to *Drosophila* males but also expressed in females in our data.

CIS and NPTIO2 groups presented a response whose enrichment has the GO terms (Figures 8 and 9) related to response to stimulus, gene expression, protein metabolism and development (BP); and enzyme, nucleic acid binding and small molecule binding (MF); DEGs in these groups are located in different cellular components but enrichment GO terms related to the membrane, endomembrane system, and macromolecular complex has found in both. Our data partially align with a previous study, which indicates that, regardless of the treatment to which *Drosophila* are subjected, upregulated genes have GO terms related to response to a stimulus, and those coding for lysozymes, cytochrome, and mitochondrial components (BROWN *et al.*, 2014).

Our data shows upregulated DEGs related to different Response to stimulus GO terms. According to GO Summary Ribbons (FlyBase (*FB2025_03, released July 24, 2025*)), the CIS group has six up-regulated DEGs with Response to stimulus GO Term: *FANCI, St4, Ir7c, PPO1, out and CG10738*. A more detailed analysis of the FlyEnrichr database shows that this set of DEGs is related to the following GO biological processes, including defense response to bacteria, oogenesis, regulation of cell proliferation, and wound healing, among others (*Supplementary Table 2*). The molecular functions of this set of DEGs are related to sulfotransferase activity, DNA polymerase binding, and hydrolase (*Supplementary Table 2*).

CIS group flies also present three upregulated lncRNA (lncRNA:CR43836, lncRNA:CR44707, lncRNA:CR45052). lncRNA:CR43836, as mentioned before, and all knowledge regarding these lncRNAs is related to regulation in transcription. Our data align with the state of the art, indicating that Cisplatin treatment induces lncRNA-mediated responses (Brown et al., 2014; Zhang et al.).

The CIS group also has DEGS related to development: *CG9503, dec, Cad88C, Cad74A, out*. The FlyEnrichr database shows that this set of DEGS is associated with the following GO biological processes: cell-cell adhesion, female germline sex determination, regulation of DNA endoreduplication, and ecdysteroid metabolic process, among others (Supplementary Table 1). These molecular functions are related to hydrolase activity and ionic binding (*Supplementary Table 2*). The simultaneous super expression of all these genes suggests that the organism is

undergoing an intense phase of development, differentiation, and tissue reorganization. They appear to be working together to coordinate the complex morphological changes that occur in the *Drosophila* body.

In the NPTIO2 group, we found out that there was upregulation in *CG1503*, *l(2)03659,* and *CG44838*. Its upregulation suggests *Drosophila* treated with 50μg/ml of TiO_2 needs to activate transport machinery to metabolize TiO_2. In case, CG44838 is a transcription factor known for signal transduction and nervous system development (Olson *et al.*, 2019) and activate *CG1503* which is a protein regulator having hydrolase activity and are related to decreased carbohydrate metabolism (Hu *et al.*, 2021), finally *l(2)03659* which is related to response to xenobiotics or metabolites mitochondrial stress-relief mechanism associated with multidrug resistance (Yeh *et al.*, 2017) due to activation in transmembrane transport mechanism.

NPTiO2 upregulated *CG11263, tut, and CG18088 DEGs*. These DEGs are associated with the regulation of negative gene expression and the piRNA metabolic process. *CG11263* is co-expressed and functions as part of the transcription machinery that enables the generation of piRNA precursors from heterochromatin while maintaining the suppression of transposon-encoded promoters and enhancers. This is also related to pupal and adult female viability (Matthews *et al.*, 2015). *CG10013* and *ord* are co-expressed and promote normal formation and maintenance of the synaptonemal complex and centromere clustering (Das *et al.*, 2016). Also, *ord* is essential for proper maintenance of sister-chromatid cohesion in both male and female meiosis. Yet, mutations in this gene cause premature separation of the sister chromatids in meiosis I and random segregation in both meiotic divisions and reduce recombination in female meiosis (Miyazaki; Orr-Weaver, 1990).

Previous data indicate that *D. melanogaster* ovaries infected with *Wolbachia sp*. exhibit upregulation of *tut, Mal-A7*, and *dany* genes, which are involved in biological processes such as cell division and recombination, and these genes are also associated with infection-related differential expression (FRANTZ *et al.*, 2023). Our data demonstrates that *Drosophila* from the NPTiO2 group exhibits upregulation only in tut but develops the same responses as flies treated with Wolbachia sp., suggesting that tut plays a key role in *Drosophila* metabolism against NPTiO2, which represses other genes.

D. melanogaster challenged with nanomaterials develops acute effects related to changes in pigmentation, survivor rate, lifespan, and genotoxicity (Zhang *et al.*, 2023). Relative to $NPTiO_2$, a study using *D. melanogaster* chronically exposed to suspensions containing 5 mg/kg, 10 mg/kg, 15 mg/kg, and 20 mg/kg $NPTiO_2$ from the embryonic period of the P0 to F3 in the adult stage, demonstrates a decrease in the total crawling distance of larvae and the total movement distance of adult males in F3. Results obtained in this study suggest disruption in the Impaired neuromuscular junction (NMJ) due to an increase expression level of genes related to response to lithium-ion response (*List*) and neuron cellular homeostasis (*Gba1a* and *hll*), and a decrease in gene expression levels of thermosensory behavior gene (*Cyp6a17*) and axon target recognition gene (*frac*) (ZHANG *et al.*, 2023). Our data, based on prolonged but not chronic exposure, corroborates these observations regarding the reduction in the expression of *frac* and *Cyp6a17*.

Our results suggest that *Aqz and CG10013,* which are DEGs upregulated by all challenged groups (*CIS, NPTIO2,* and *CIS_NPTIO2*), may play a significant role in the fly response to cisplatin and TiO_2 nanoparticles. Also, the upregulation of these DEGs by all treated groups indicates that ribosomal production metabolism is affected by these treatments.

Our data suggest that changes in metabolism occur in the CIS_NPTIO2 group, primarily affecting cell division metabolism, which is significantly impacted by the combined use of Cisplatin and $NPTiO_2$. Flies in this group exhibit no statistical difference in survival (Figure 1). Despite the protein intake during treatment, which leads to cell division and gametogenesis (Britton; Edgar, 1998), a strong quiescence in cell division metabolism is observed.

These results suggest that the combined use of Cisplatin and $NPTiO_2$ is effective in reducing the expression level and in promoting quiescence in dividing cells. Our *in vivo* study suggests that the combination of these substances may affect cell division in *Drosophila* treated concomitantly with cisplatin and TiO_2 nanoparticles, which could help treat cancers for which cisplatin alone does not achieve the desired effect.

References:

ADAMS, MARK D. The Genome Sequence of Drosophila melanogaster. **Science**, v. 5461, p. 2185–2195, 2000.

ADIBZADEH, R. *et al.* Combination therapy with TiO2 nanoparticles and cisplatin enhances chemotherapy response in murine melanoma models. **Clinical and Translational Oncology**, v. 23, n. 4, p. 738–749, abr. 2021.

ANDERS, Simon; PYL, Paul Theodor; HUBER, Wolfgang. HTSeq—a Python framework to work with high-throughput sequencing data. **Bioinformatics**, v. 31, n. 2, p. 166–169, 15 jan. 2015.

BARMO, Cristina *et al.* In vivo effects of n-TiO2 on digestive gland and immune function of the marine bivalve Mytilus galloprovincialis. **Aquatic Toxicology**, v. 132–133, p. 9–18, maio 2013.

BASTIDE, Héloïse *et al.* A Variable Genetic Architecture of Melanic Evolution in *Drosophila melanogaster*. **Genetics**, v. 204, n. 3, p. 1307–1319, 1 nov. 2016.

BRENT, M. M.; OSTER, I. I. Nutritional Substitution- a new approach to microbial control for Drosophila cultures. p. 155–157, 1974.

BRITTON, Jessica S.; EDGAR, Bruce A. Environmental control of the cell cycle in Drosophila: nutrition activates mitotic and endoreplicative cells by distinct mechanisms. **Development**, v. 125, n. 11, p. 2149–2158, 1 jun. 1998.

CHEN, Zijing; MONTELL, Craig. A Family of Auxiliary Subunits of the TRP Cation Channel Encoded by the Complex InaF Locus. **Genetics**, v. 215, n. 3, p. 713–728, 1 jul. 2020.

CRIDLAND, Julie M.; BEGUN, David J. Male-derived transcripts isolated from the mated female reproductive tract in *Drosophila melanogaster*. **G3: Genes, Genomes, Genetics**, v. 13, n. 11, p. jkad202, 1 nov. 2023.

DAS, Arunika *et al.* Spindle Assembly and Chromosome Segregation Requires Central Spindle Proteins in Drosophila Oocytes. **Genetics**, v. 202, n. 1, p. 61–75, 1 jan. 2016.

GARCÍA SAR, Daniel *et al.* Relationships between cisplatin-induced adducts and DNA strand-breaks, mutation and recombination in vivo in somatic cells of Drosophila melanogaster, under different conditions of nucleotide excision repair. **Mutation Research/Genetic Toxicology and Environmental Mutagenesis**, v. 741, n. 1–2, p. 81–88, jan. 2012.

GARLOVSKY, Martin D.; SANDLER, Jessica A.; KARR, Timothy L. Functional Diversity and Evolution of the Drosophila Sperm Proteome. **Molecular & Cellular Proteomics**, v. 21, n. 10, p. 100281, out. 2022.

GHOSH, Sumit. Cisplatin: The first metal based anticancer drug. **Bioorganic Chemistry**, v. 88, p. 102925, jul. 2019.

GROEN, Christopher M. *et al.* Genetic Reduction of Mitochondria Complex I Subunits is Protective against Cisplatin-Induced Neurotoxicity in Drosophila. **The Journal of Neuroscience**, v. 42, n. 5, p. 922, 2 fev. 2022.

HU, Yanhui *et al.* FlyRNAi.org—the database of the Drosophila RNAi screening center and transgenic RNAi project: 2021 update. **Nucleic Acids Research**, v. 49, n. D1, p. D908–D915, 8 jan. 2021.

JOVANOVIĆ, Boris; CVETKOVIĆ, Vladimir J.; MITROVIĆ, Tatjana Lj. Effects of human food grade titanium dioxide nanoparticle dietary exposure on Drosophila melanogaster survival, fecundity, pupation and expression of antioxidant genes. **Chemosphere**, v. 144, p. 43–49, fev. 2016.

KARASAWA, Takatoshi; STEYGER, Peter S. An integrated view of cisplatin-induced nephrotoxicity and ototoxicity. **Toxicology Letters**, v. 237, n. 3, p. 219–227, set. 2015.

KIRKLAND, David *et al.* A weight of evidence review of the genotoxicity of titanium dioxide (TiO2). **Regulatory Toxicology and Pharmacology**, v. 136, p. 105263, dez. 2022.

KULESHOV, Maxim V. *et al.* modEnrichr: a suite of gene set enrichment analysis tools for model organisms. **Nucleic Acids Research**, v. 47, n. W1, p. W183–W190, 2 jul. 2019.

LI, Xiao *et al.* Cdk8 attenuates lipogenesis by inhibiting SREBP-dependent transcription in *Drosophila*. **Disease Models & Mechanisms**, v. 15, n. 11, p. dmm049650, 1 nov. 2022.

LIU, Sai-Lan *et al.* TIMELESS confers cisplatin resistance in nasopharyngeal carcinoma by activating the Wnt/β-catenin signaling pathway and promoting the epithelial mesenchymal transition. **Cancer Letters**, v. 402, p. 117–130, ago. 2017.

LUSHCHAK, Oleh; STRILBYTSKA, Olha; STOREY, Kenneth B. Gender-specific effects of pro-longevity interventions in Drosophila. **Mechanisms of Ageing and Development**, v. 209, p. 111754, jan. 2023.

MACKAY, Trudy F. C. *et al.* The Drosophila melanogaster Genetic Reference Panel. **Nature**, v. 482, n. 7384, p. 173–178, fev. 2012.

MATSUOKA, Shinya *et al.* Adipocyte Metabolic Pathways Regulated by Diet Control the Female Germline Stem Cell Lineage in Drosophila melanogaste. **Genetics**, v. 206, n. 2, p. 953—971, jun. 2017.

MATTHEWS, Beverley B. *et al.* Gene Model Annotations for Drosophila melanogaster: Impact of High-Throughput Data. **G3 Genes|Genomes|Genetics**, v. 5, n. 8, p. 1721–1736, 1 ago. 2015.

MIYAZAKI, W.; ORR-WEAVER, T. Genetic and molecular analysis of orientation disrupter (ord). 1990.

MOHAMED, Hanan Ramadan Hamad. Estimation of TiO2 nanoparticle-induced genotoxicity persistence and possible chronic gastritis-induction in mice. **Food and Chemical Toxicology**, v. 83, p. 76–83, set. 2015.

MOMBACH, Daniela Moreira *et al.* Molecular and biological effects of Cisplatin in Drosophila. **Comparative Biochemistry and Physiology Part C: Toxicology & Pharmacology**, v. 252, p. 109229, 2022.

MORRISON, Julie L. *et al.* A lock-and-key model for protein–protein interactions. **Bioinformatics**, v. 22, n. 16, p. 2012–2019, 15 ago. 2006.

OLSON, John M. *et al.* Expression-Based Cell Lineage Analysis in Drosophila Through a Course-Based Research Experience for Early Undergraduates. **G3 (Bethesda, Md.)**, v. 9, n. 11, p. 3791–3800, 5 nov. 2019.

ÖZTÜRK-ÇOLAK, Arzu *et al.* FlyBase: updates to the Drosophila genes and genomes database. **Genetics**, v. 227, n. 1, p. iyad211, 1 maio 2024.

POSPISILIK, J. Andrew *et al.* Drosophila Genome-wide Obesity Screen Reveals Hedgehog as a Determinant of Brown versus White Adipose Cell Fate. **Cell**, v. 140, n. 1, p. 148–160, jan. 2010.

PROKUPEK, Adrianne *et al.* AN EVOLUTIONARY EXPRESSED SEQUENCE TAG ANALYSIS OF DROSOPHILA SPERMATHECA GENES. **Evolution**, v. 62, n. 11, p. 2936–2947, nov. 2008.

ROBINSON, Mark D.; MCCARTHY, Davis J.; SMYTH, Gordon K. edgeR : a Bioconductor package for differential expression analysis of digital gene expression data. **Bioinformatics**, v. 26, n. 1, p. 139–140, 1 jan. 2010.

SUN, Zhipeng; NYSTUL, Todd G.; ZHONG, Guohua. Single-cell RNA sequencing identifies eggplant as a regulator of germ cell development in Drosophila. **EMBO reports**, v. 24, n. 10, p. e56475, 9 out. 2023.

WANI, Mohammad Rafiq; SHADAB, Ggha. Titanium dioxide nanoparticle genotoxicity: A review of recent in vivo and in vitro studies. **Toxicology and Industrial Health**, v. 36, n. 7, p. 514–530, jul. 2020.

WINGETT, Steven W.; ANDREWS, Simon. FastQ Screen: A tool for multi-genome mapping and quality control. **F1000Research**, v. 7, p. 1338, 17 set. 2018.

YEH, Johannes T. H. *et al.* eUnaG: a new ligand-inducible fluorescent reporter to detect drug transporter activity in live cells. **Scientific Reports**, v. 7, n. 1, p. 41619, 8 fev. 2017.

ZHANG, Xing *et al.* Chronic exposure to titanium dioxide nanoparticles induces deficits of locomotor behavior by disrupting the development of NMJ in Drosophila. **Science of The Total Environment**, v. 888, p. 164076, ago. 2023.

ZHONG, Guocai *et al.* A reversible RNA on-switch that controls gene expression of AAV-delivered therapeutics in vivo. **Nature Biotechnology**, v. 38, n. 2, p. 169–175, fev. 2020.